SCISPACE
formerly Typeset

Open access • Journal Article • DOI:10.1063/1.1135841

Construction of a Cerenkov light source. — Source link

G. B. Rothbart, J. C. Sheppard, Melvin A. Piestrup, R. A. Powell ...+2 more authors

Institutions: Stanford University

Published on: 01 Apr 1979 - Review of Scientific Instruments (American Institute of Physics)

Topics: Optical radiation and Linear particle accelerator

Related papers:

- Synchrotron radiation optics in the short-pulse limit: design implications for the SLAC Linac Coherent Light Source (LCLS)
- Projected performance of rf-linac-driven free-electron lasers in the extreme-ultraviolet spectral region☆
- Velociraptor: LLNL's Precision Compton Scattering Light Source
- Infrared (IR) vs. X-ray power generation in the SLAC Linac Coherent Light Source (LCLS)
- New light source in a submillimeter to millimeter range using the coherent radiation from the single-bunch electron beam at ISIR

Share this paper:

View more about this paper here: https://typeset.io/papers/construction-of-a-cerenkov-light-source-4kojr62uhy

SLAC-PUB-2210
October 1978
(I)

CONSTRUCTION OF A CERENKOV LIGHT SOURCE*

G. B. Rothbart, J. C. Sheppard, M. A. Piestrup, R. A. Powell, R. H. Pantell
Department of Electrical Engineering
Stanford University, Stanford, CA 94305

and

R. A. Gearhart
Stanford Linear Accelerator Center
Stanford University, Stanford, CA 94305

ABSTRACT

A radiation source has been developed and implemented from Cerenkov emission that is intended to provide an intense continuum from the infrared to 600Å. Parasitic use of the primary electron beam at the Stanford Linear Accelerator Center (SLAC) together with a novel optical geometry for light collection can give a focused and tunable ultraviolet beam with 10^4 KW/m^2-steradian brightness, 10^{-2} spectral purity, and with the pulsed, 5 picosecond time structure of the SLAC electron beam. Measurements of the emission characteristics in the visible part of the spectrum correlate closely with the predicted performance.

(Submitted to Nucl. Instr. Methods)

*Research supported by the National Science Foundation and the Department of Energy contract no. EY-76-C-03-0515.

I. Introduction

We have developed and are in the process of testing a unique source of vacuum ultraviolet (VUV) radiation where, prior to this time, few radiation sources in this portion of the spectrum existed, particularly for wavelengths shorter than 1000Å. This source of infrared-to-600Å radiation is intense, simple for an experimenter to use, comparable in flux to synchrotron radiation on a time averaged basis, and pulsed on a microsecond time scale.

The method uses Cerenkov radiation together with an optical geometry that allows the entire Cerenkov cone to be collected and single frequencies focused to a point. Figure 1 is a sketch of the major features of the experimental configuration. Cerenkov radiation is generated by passing the primary electron beam at SLAC through 7 meters of helium gas at low pressure.

The SLAC electron beam[1] on the C-beamline, which is where our gas cell is located, is characterized by 5 psec (FWHM) pulses, separated by 350 psec, lasting 1.6 μsec with 10 to 60 of the 1.6 μsec pulses per second. Electron current averaged over the 1.6 μsec time interval is normally between 1 and 4 mA, and the particle energy is between 10 and 21 GeV. Since Cerenkov radiation is only velocity sensitive, changes in beam energy in this high energy range do not affect optical production. The beam emittance at SLAC is 0.1 mm-mrad and the beam diameter at our cell is 2 mm FWHM. Therefore, the divergence observed at the same point is 0.050 mrad FWHM.

The forward cone of radiation is incident upon a specially designed and fabricated mirror. This mirror point focuses a conical wavefront of

7 mrad opening angle, with a 21.74 meter focal length. Since helium is dispersive for wavelengths close to its 584Å resonance, only a narrow frequency bandwidth is focused to a small spot. Therefore the combined characteristics of the mirror and the gas allow frequency selection without the use of a monochromator, eliminating as much as 20 db additional attenuation.

As illustrated in Figure 1, the focal point is located just above ground level, over the earth and concrete cover for the accelerator. The optical beam arrives at this point using a 45° deflecting mirror and a helium-filled light extraction tube. Figure 2 details the optics at the focus, which are located in an experimenter's trailer. The focal plane is at the position of the 3 mm iris.

II. System Design

A. Parameter Selection

Equations of Cerenkov production[2] are the basis for the design of the VUV source. The opening angle, θ_c, of the conical shell of emission is given by

$$\cos\theta_c = \frac{1}{n\beta}\left(1 - \frac{n^2-1}{2}\frac{\hbar\omega}{mc^2}\right) \qquad (1)$$

where

β = v/c is the electron beam velocity

n = index of refraction

$\hbar\omega$ = photon energy

mc^2 = electron beam energy

The second term, due to kinematical recoil, is negligible at SLAC energies, reducing Eq. (1) to the simple form

$$\theta_c \cong \sqrt{2(n-1)} \tag{2}$$

where the error in this approximation is 2×10^{-6}.

Refractive index for helium is dispersive, and in the spectral region of interest depends primarily on the single resonance at $584\text{Å} = \lambda_0$:

$$n-1 = 35 \times 10^{-6} \frac{P}{1-(\lambda_0/\lambda)^2} \tag{3}$$

where P is the pressure of helium in atmospheres at standard temperature. Combining Eqs. (2) and (3) gives the relationship among θ_c, P, and λ:

$$\theta_c = 8.48 \sqrt{\frac{P}{1-(\lambda_0/\lambda)^2}} \quad \text{mrad} \tag{4}$$

The collection mirror is designed to bring to a point focus only the radiation which is emitted at an opening angle of θ_0. Radiation emitted at other angles, θ, is focused in the image plane to rings of diameter d,

$$d = 2f\,|\theta - \theta_0| \tag{5}$$

where f ≡ focal length of the mirror. An iris in the focal plane occludes radiation not focused to a point. That is, the optical system is designed to act as a filter of angles, picking out θ_0 from the continuum of Cerenkov emission angles. Figure 3 is a schematic representation of the image forming process of the collection mirror. From Eq. (4) it is seen that for a fixed pressure only a single wavelength will be focused, corresponding to the wavelength for which $\theta_c = \theta_0$:

$$\lambda = \lambda_0 \left[1 - P\left(\frac{8.48}{\theta_0}\right)^2 \right]^{-1/2} \tag{6}$$

Therefore, by controlling pressure the wavelength can be tuned.

The bandwidth associated with this system is

$$\frac{d\lambda}{\lambda} = \frac{d\theta_0}{\theta_0}\left[\left(\frac{\lambda}{\lambda_0}\right)^2 - 1\right] \tag{7}$$

where $d\theta_0$ is about 70 μrad. Uncertainty $d\theta_0$ in the emission angle that is brought to a focus is determined by the quality of the collection mirror, diffraction effects, and electron beam divergence and scattering in the cell.

Photons generated per unit frequency $\frac{dN}{d\omega}$, neglecting absorption and reflection losses in the system, is given by

$$\frac{dN}{d\omega} = 2.44 \times 10^{-11} L \theta_c^2 \tag{8}$$

where L is the path length in meters over which radiation is produced and collected. At the gas pressure for which the light is focused $\theta_c = \theta_0$, so that at the focus $\frac{dN}{d\omega}$ is independent of frequency and does not depend upon which gas is used in the cell.

The independent design parameters are the Cerenkov gas, the interaction length L, and focusing angle of the mirror θ_0. Helium gas was selected as the primary medium because it can provide radiation to wavelengths as short as 600Å, and the interaction length was determined by the drift space available at SLAC in close proximity to an overhead penetration. The remaining parameter is θ_0.

With θ_0 specified, it is possible to calculate the light intensity collection, wavelength as a function of pressure, and spectral purity.

Collected light is related to photon production by the known absorption constant of the gas and the reflectivity of the various reflecting surfaces.

A computer code has been written to examine the characteristics of a Cerenkov source for various θ_0. The program prepares plots of gas pressure required at each wavelength, intensity vs. wavelength, and spectral purity vs. wavelength. It was found that collection angles in the range of 4 - 10 mrad produce optimal flux within a pressure range constrained to less than one atmosphere. Smaller angles result in less photon production (as given by Eq. (8)), while larger angles require higher pressures and therefore introduce appreciable absorption.

Collection at any given wavelength could be maximized by a proper choice of θ_0, and in the range of λ = 600Å to 2000Å, this value of θ_0 is from 4 to 10 mrad. Fortunately, the peak in λ is broad, and by choosing θ_0 in the mid-range production is uniform within a decade over the entire VUV spectrum.

In addition, θ_0 = 4 mrad would produce a spot diameter at the collection mirror of 56 mm, while the order of a 25 mm diameter center hole is required for elecron beam passage, thereby losing 25% of the produced radiation. On the other hand, θ_0 = 10 mrad would require fabrication of a large diameter mirror which has both technical and economic disadvantages. An angle θ_0 = 7.0 mrad was chosen to yield the best flux over the range of interest, while also giving reasonable dimensions for the collection mirror.

The effective path length L, which is the length of electron travel for which the Cerenkov radiation is reflected from the mirror, is less than the total path length L_0 because of the hole in the collection mirror.

(See Figure 7.) Namely,

$$L = L_o - r_h / \sin\theta_c \tag{9}$$

where r_h is the radius of the hole in the mirror. Using a 3 mm iris in the focal plane, the corresponding $d\theta$, which is given by the iris aperature divided by the mirror focal length, 21.74 m, will be 138.0 μrad. For this value of $d\theta$ and for $\theta_c = \theta_0 = 7.0$ mrad, $L_0 = 7.0$ m, and $r_h = 15.9$ mm, L = 4.7 m; Eqs. (7) and (8) become

$$\frac{d\lambda}{\lambda} = 1.97\left[\left(\lambda/\lambda_0\right)^2 - 1\right]\% \tag{10}$$

$$\frac{\partial N}{\partial E} = 8.60 \text{ per electron per eV} \tag{11}$$

Figure 4 is a plot of spectral purity, and Figure 5 shows both the ideal flux at the focus (i.e. the flux neglecting losses), and the flux where self-absorption and mirror reflection losses are included.

Neglecting losses, the Cerenkov source in the 10 eV - 20 eV range emits 2×10^9 - 0.6×10^{11} photons/mA-pulse through a 3 mm iris at the focus. For typical pulse rates of 10 per second and electron currents of 5 mA, 10^{11} - 3×10^{12} photons/sec are generated, including the effects of self-absorption in the gas. The two mirror reflections account for 80% loss each, so that the photon rate present at the focus is $(0.25 - 10)\times10^{10}$ photons/sec.

B. Helium Cell Design and Fabrication

The cell is designed and fabricated to contain helium, encapsulate the collection mirror and 45° diagonal mirror, and allow extraction of light vertically through the earth and concrete cover of the accelerator. Vacuum welding, pumping ports, thermocouple vacuum gauges, access ports,

alignment motors, and mechanical support structures were major considerations.

The body of the cell is aluminum (alloy 6061 - T6), which for the larger tubes were rolled from flat plate and then heli-arced. All welding joints were of the full "penetration" type to avoid the existence of trapped gas volumes.

The cell was extensively leak-checked and upon its completion proved to have no helium leak larger than 2×10^{-12} liter/sec (the noise level of the leak checking equipment). It was then cleaned for high-vacuum, installed at SLAC, and precision aligned in both the vertical and horizontal to the electron beam to within 0.25 mm. Figure 6 is a photograph of the completed cell in position prior to the installation of the vertical extraction tube.

C. Mirror Design

The collection mirror is a special surface[3] whose function is to focus conical wavefronts of a given conical angle, generated along a line, to a point. The cone angle is 7.0 mrad, the focal length of the mirror is 21.74 meters, and the diameter of the mirror is 15.2 cm. Thus, not only is the shape non-spherical, the f-number of f/150 and the mirror aperture are exceedingly large.

The mirror surface is best described by considering a cross-sectional cut through the center of the mirror (see Figure 7). The curvature of the mirror is just that of a "Gothic arch," i.e. an arch formed by two circles of equal radii and displaced centers. Rotating this curve about the electron beam axis produces the reflecting surface we require.

The equation of the mirror surface is

$$S = f\sqrt{3+\cos^2\theta_0} - 2f\sqrt{1-\left(\frac{r-f\sin\theta_0}{2f}\right)^2} \qquad (12)$$

where

s = sagitta of the surface

f = focal length (21.74 meters)

θ_0 = collection angle (7 mrad)

r = radial distance from the mirror center

Eq. (12) is very well approximated by

$$S = \frac{r^2}{4f} + \frac{r\theta_0}{2}$$

$$= 1.15 \times 10^{-5} r^2 + 0.0035 r \qquad (13)$$

where r and s are in mm.

Figure 8 is a plot of this mirror surface. The mirror is a 2.54 cm thick aluminum blank with an electroplated nickel substrate. After grinding and polishing, the mirror was plated with a platinum reflecting surface. A 3.18 cm center hole allows the electron beam to pass through the mirror.

A He-Ne laser was used as a light source to measure the spot size at the focal point of the mirror. The observed FWHM dimension of 0.7 mm was attributable to the divergence of the laser. Thus, for 7000Å the circle of confusion due to mirror irregularity is less than 0.7 mm.

D. Detector Considerations

Quantitative measurements in the visible are made with a photodiode detector, and in the UV with a photodiode or photomultiplier tube in combination with a wavelength shifter (WLS).

The number of photons arriving at the detector is in the range of 10^8 - 10^{10} per milliampere per pulse. Using sodium salycilate as a WLS provides a quantum efficiency of about 0.15 and fluoresces at 2.4 eV. Thus, the peak power from the WLS is 4 - 400 μW per mA of electron beam

current. At this frequency, the photodiode will generate about 0.3 mA of current per mW of input power, so that the voltage into 50Ω is 60 - 6000 μV per mA of electron beam current. The thermal noise due to a 1 MHz handpass and 50Ω impedence is about 1 μV, giving a signal to noise ratio of 60 - 6000.

III. Measurements of Visible Cerenkov Light Using Air in the Cell

The first test of the system collected and observed visible Cerenkov light at the focus using a 20 GeV, 10pps, 5 mA peak current electron beam passing through air at pressures in the range of 45 - 80 torr. The focused light was viewed on a ground glass diffuser.

Dispersion in air was observed as a "rainbow effect." For pressures below 63.7 torr, concentric rings of colors were observed with red at the larger radii and blue and violet at the smaller radii. At 63.7 torr the ring pattern collapsed to a bluish-white spot. As the pressure was increased further, concentric rings again formed with blue and violet at the outside and red at the inside. This result is expected for normal dispersion, wherein n and θ_0 decrease with increasing λ. The ring width in the visible was measured to be about 2 mm for a mean ring diameter of 30 mm, at a pressure of 51.7 torr.

A. Ring Diameter as a Function of Cell Pressure

The first measurement concerned the mean diameter of the ring as a function of air pressure in the cell. Rays impinging on the mirror at an angle θ are focused at a radial distance R from the focal point given by

$$R = f\,|\theta - \theta_0| \tag{14}$$

From Eqs. (2) and (14) we obtain for the ring diameter D

$$D = 2f \left| \sqrt{2(n-1)_o P} - \Theta_o \right| \qquad (15)$$

where $(n-1)_0$ is (n-1) measured at STP and P is the pressure in atmospheres. For air, $(n-1)_0 = 292.4 \times 10^{-6}$ at 5500Å.

The measurement was made by introducing a small leak into the cell at a carefully measured rate, and then recording the mean ring diameter as a function of time. Pressure measurements were then corrected to standard temperature. Data are plotted in Figure 9 together with the theoretical curve of Eq. (15). The very fine agreement demonstrates the validity of Eq. (15), the correct optical properties of the collection mirror, and verifies that the design values of θ_0 and f are properly incorporated in the mirror surface.

When the light is focused, the predicted value for n-1, as given by Eq. (2), is

$$n-1 = \Theta_o^2/2 = 24.5 \times 10^{-6}$$

where $\theta_0 = 7.0$ mrad. A comparison with the measured value for n-1 can be obtained from Figure 9. From the data points, the pressure at the focus is 63.3 ± 0.3 torr. This gives

$$(n-1) = (n-1)_o \frac{(63.3 \pm 0.3)}{760} = (24.4 \pm 0.1) \times 10^{-6}$$

which equals the theoretical value to within the experimental uncertainty.

Eq. (15) may also be used to predict the effects of dispersion. The spread in radii of the visible ring, ΔR, is

$$\Delta R = R(\lambda_2) - R(\lambda_1)$$
$$= f\sqrt{2P}\left[\sqrt{n(\lambda_2)-1} - \sqrt{n(\lambda_1)-1}\right] \qquad (16)$$
$$= 1.50 \text{ mm at } 50 \text{ torr}$$

for λ_1 = 4000Å and λ_2 = 7000Å. Quantitative measurement using a photodiode array gave a 2 mm width to the visible ring which is in reasonable agreement with Eq. (16).

B. Spot Size at the Focus

A linear photodiode array was used to measure light intensity as a function of radius for a focused spot. The array consisted of 512 elements space 25μ apart. Figure 10 shows the light intensity is a function of the radius when the light is focused to its minimum size which, in air, corresponds to a pressure of 63.7 torr. The FWHM pressure is measured to be 2.7 mm.

C. Power Measurements

Output power has been measured as a function of pressure for the air filled cell. The power expected per electron is given by[4]

$$IP = 2\pi^2 \alpha \hbar c \int_{\lambda_1}^{\lambda_2} L(\lambda) \sin^2\theta_c(\lambda) \frac{d\lambda}{\lambda} \qquad (17)$$

where

α = fine structure constant ≃ 1/137

ℓ_1, ℓ_2 = wavelength cut-offs

For small angles, $\sin\theta_c \simeq \theta_c \simeq \sqrt{2(n-1)_0 P}$, so that the power can be expressed in terms of the observed pressure, P.

The measurement was made by allowing the light to emerge from the cell

through a lucite window, reflected into the horizontal with a 45° aluminum mirror, and focused onto a photodiode using a crown glass lens of long focal length. The photodiode response cuts off at wavelengths shorter than 1.05μm, and the lucite sharply cuts off wavelengths shorter than 0.35μm. Thus, λ_1 and λ_2 are determined, and we obtain

$$IP = 124\left(7.0 - \frac{.657}{\sqrt{P}}\right)P \qquad (18)$$

where IP is in mW per mA of beam current, and P is in atmospheres. Eq. (18) is then corrected for loss on each of two platinum mirrors (44.3% per reflection), loss through reflections at the lucite surfaces (92% transmission), loss at the aluminum mirror (90% reflection), and loss through the lens. The expected power into the detector is therefore 15.3% of that expressed in Eq. (18).

Figure 11 presents the measured power into the photodiode as a function of the cell pressure, along with the predicted power obtained from Eq. (18) and corrected as noted above. The data are 6.1% higher than theory, which may be due to poor calibration of the beam current toroid in the primary electron beam, or tolerance in the nominal response curve of the photodiode as specified by the manufacturer.

D. Polarization

Cerenkov radiation is radially polarized,[4] and rings in the focal plane should possess the same polarization. Using a polarizer, the transmitted intensity of a section of the ring was measured as a function of polarizing angle. The results are shown in Figure 12. The data conform to the expected $\cos^2\theta_p$ dependence very closely (where $\theta_p = 0$ corresponds to the direction of polarization), although it appears that polarization is incomplete. In fact,

the polarizer does not extinguish radiation at $\theta_p = 90°$ for wavelengths longer than about 8000Å. A photospectrometric measurement of the transmission curve of the polarizer, together with the response curve of the detector enable a calculation of the intensity for $\theta_p = 90°$ expressed as a fraction of the intensity for $\theta_p = 0°$. This ratio is predicted to be 14.8% and we measure 13% ± 1%. Thus, the transmitted light for $\theta_p = 90°$ is not due to incomplete polarization, but rather due to light transmitted to the detector in the spectral range where the polarizer is ineffective.

IV. Comments

All tests of the Cerenkov source made in the visible portion of the spectrum indicated proper functioning of the optical collection and focusing systems. Tests made in the UV and VUV are in progress and those results will report the realizable quality of this device as a VUV source of radiation.

V. Acknowledgements

The authors wish to mention the participation of those at Stanford and SLAC who contributed their talents toward the progress of this work. We thank Mr. K. Shill of Worthwhile Products for the entire mechanical design of the cell; F. Zweers, J. Grim, H. Kent, and B. Bubna for fabrication of the cell; Mr. B. Zatlin of Applied Optics and Dr. R. Benjamin of Bell and Howell for fabrication and preparation of the mirrors; Mr. B. Smith, E. Keyser, and F. Halbo of SLAC for installation of the cell and experimental trailer; Dr. B. Sukiennicki for his design of the accelerator

protection devices; Dr. J. Murray for many useful discussions of the physics and engineering aspects of this work; and Drs. R. Mozley and W. K. H. Panofsky for approving and arranging beamtime and SLAC support for this research.

REFERENCES

1. Neal, R. B., editor, The Stanford Two-Mile Accelerator, W. A. Benjamin, Inc., 1968.

2. Jelley, J. V., Cerenkov Radiation and its Application, Pergamon Press, 1958, Los Angeles, p. 19.

3. Jelley, op. cit., pp. 162-165.

4. Jelley, op. cit., pp. 19-22.

FIGURE CAPTIONS

Figure 1. Overview of the experimental configuration.

Figure 2. Experimental configuration in laboratory area. The radiation is brought to a focus in the plane of the 3.0 mm iris. A wavelength shifter is used to translate the ultraviolet emission into the visible portion of the spectrum. The purpose of the 3.25 mm iris is to eliminate most of the radiation that is scattered off the walls of the vertical pipe.

Figure 3. Electrons propagate along the z-axis emitting photons λ_0, λ_1, λ_2, at angles θ_0, θ_1, θ_2 such that $\theta_1 < \theta_0 < \theta_2$. For $\theta_0 \equiv$ design angle of the mirror, λ_0 is point-focused while λ_1 and λ_2 are focused to rings in the focal plane. An iris placed in the focal plane blocks radiation emitted at angles other than θ_0.

Figure 4. Bandwidth of the radiation at the focus as a function of wavelength, using He gas in the cell.

Figure 5. Photons generated at the focus per electron beam pulse, per milliampere of electron beam current as a function of wavelength, using He gas.

Figure 6. Cerenkov cell in place in the SLAC C-line prior to the installation of the vertical extraction tube and radiation shielding.

Figure 7. Design of the focusing mirror.

Figure 8. Sagitta of collection mirror designed to focus 7 mrad cones with focal length of 21.74 meters.

Figure 9. Mean ring diameter as a function of the pressure of air in the cell, normalized to standard temperature. The focus is expected to occur for 63.7 torr.

Figure 10. Photodiode array response to focused visible Cerenkov light from air at 63.7 torr pressure.

Figure 11. Total power in the visible as a function of air pressure.

Figure 12. Polarization of Cerenkov light at a section of the Cerenkov ring. Light is not completely extinguished at 90° due to tapering performance of the analyzing polarizer at wavelengths longer than 8000Å.

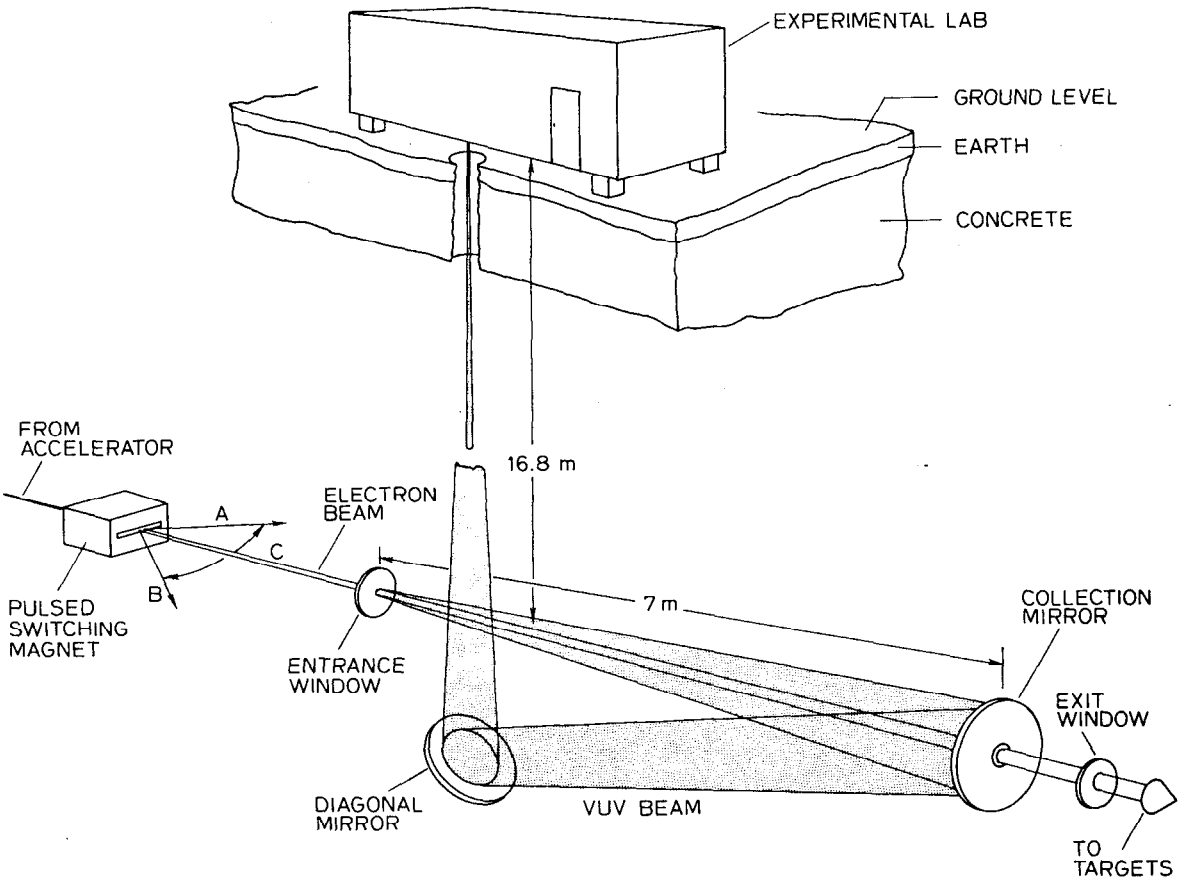
EXPERIMENTAL LAB
GROUND LEVEL
EARTH
CONCRETE
16.8 m
FROM
ACCELERATOR
A
B
C
ELECTRON
BEAM
PULSED
SWITCHING
MAGNET
ENTRANCE
WINDOW
7 m
COLLECTION
MIRROR
EXIT
WINDOW
DIAGONAL
MIRROR
VUV BEAM
TO
TARGETS

Fig. 1

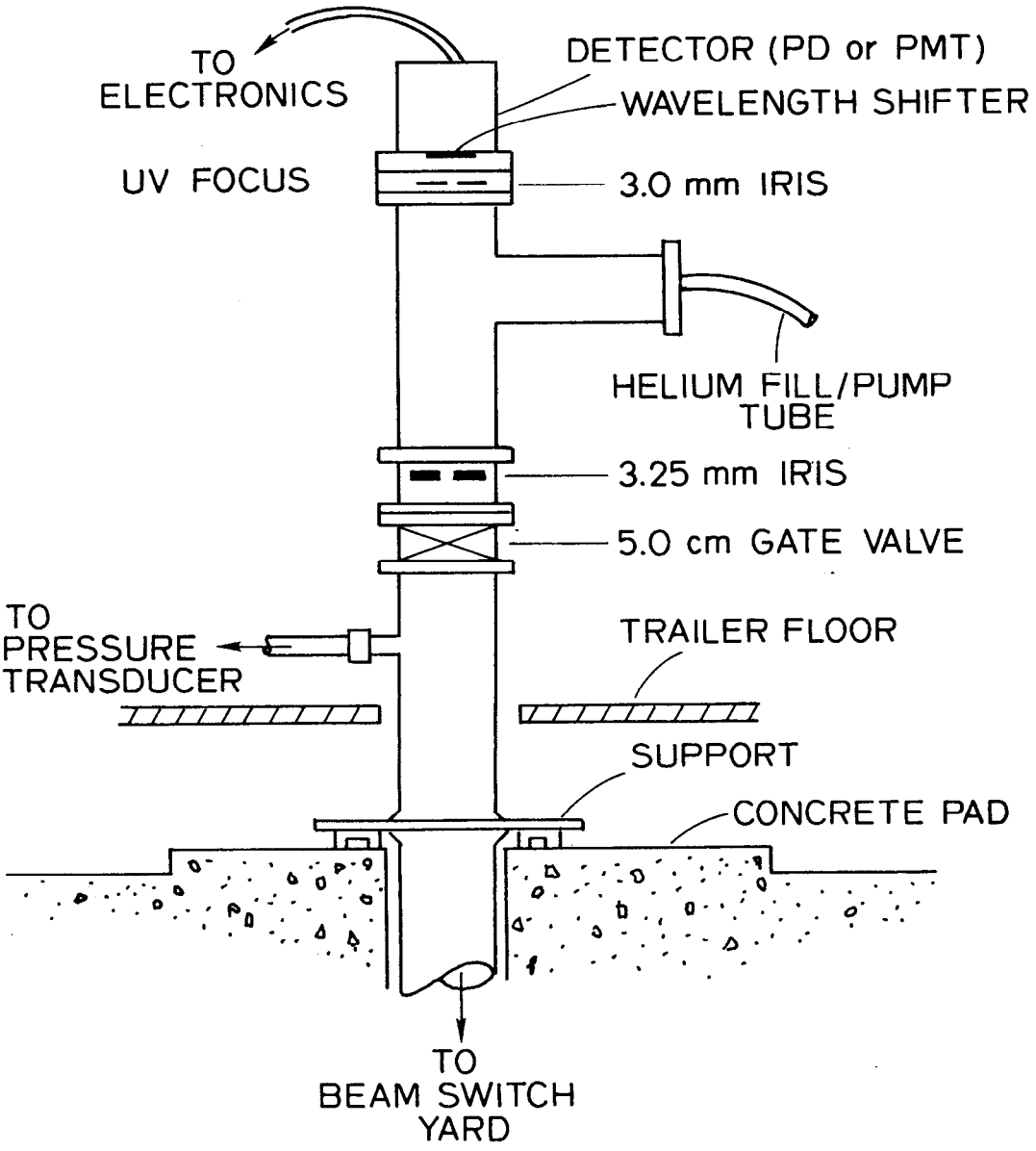
TO
ELECTRONICS
DETECTOR (PD or PMT)
WAVELENGTH SHIFTER
UV FOCUS
3.0 mm IRIS
HELIUM FILL/PUMP
TUBE
3.25 mm IRIS
5.0 cm GATE VALVE
TO
PRESSURE
TRANSDUCER
TRAILER FLOOR
SUPPORT
CONCRETE PAD
TO
BEAM SWITCH
YARD

Fig. 2

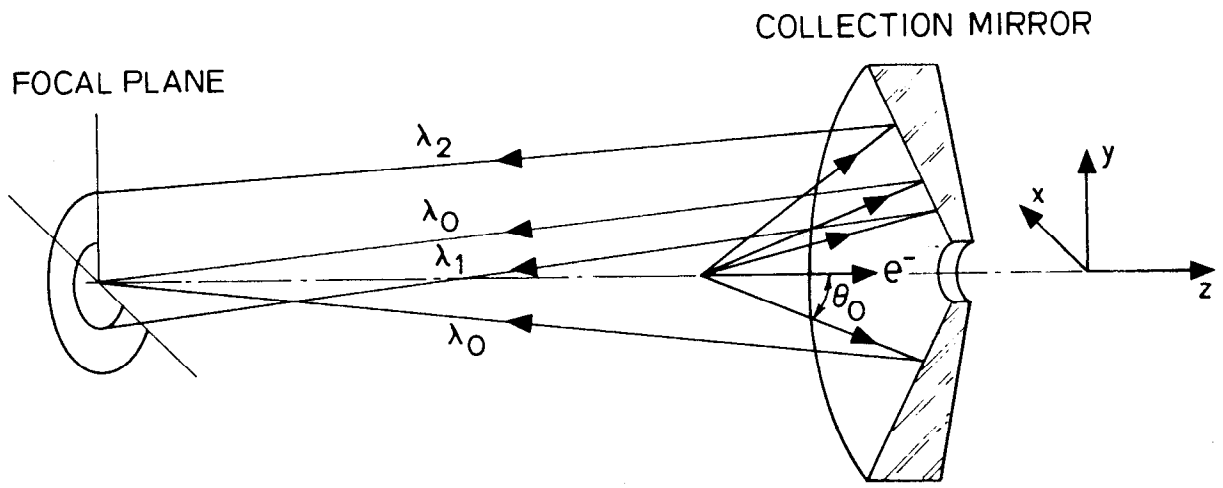
COLLECTION MIRROR
FOCAL PLANE
λ_2
λ_0
λ_1
λ_0
e^-
θ_0
y
x
z

Fig. 3

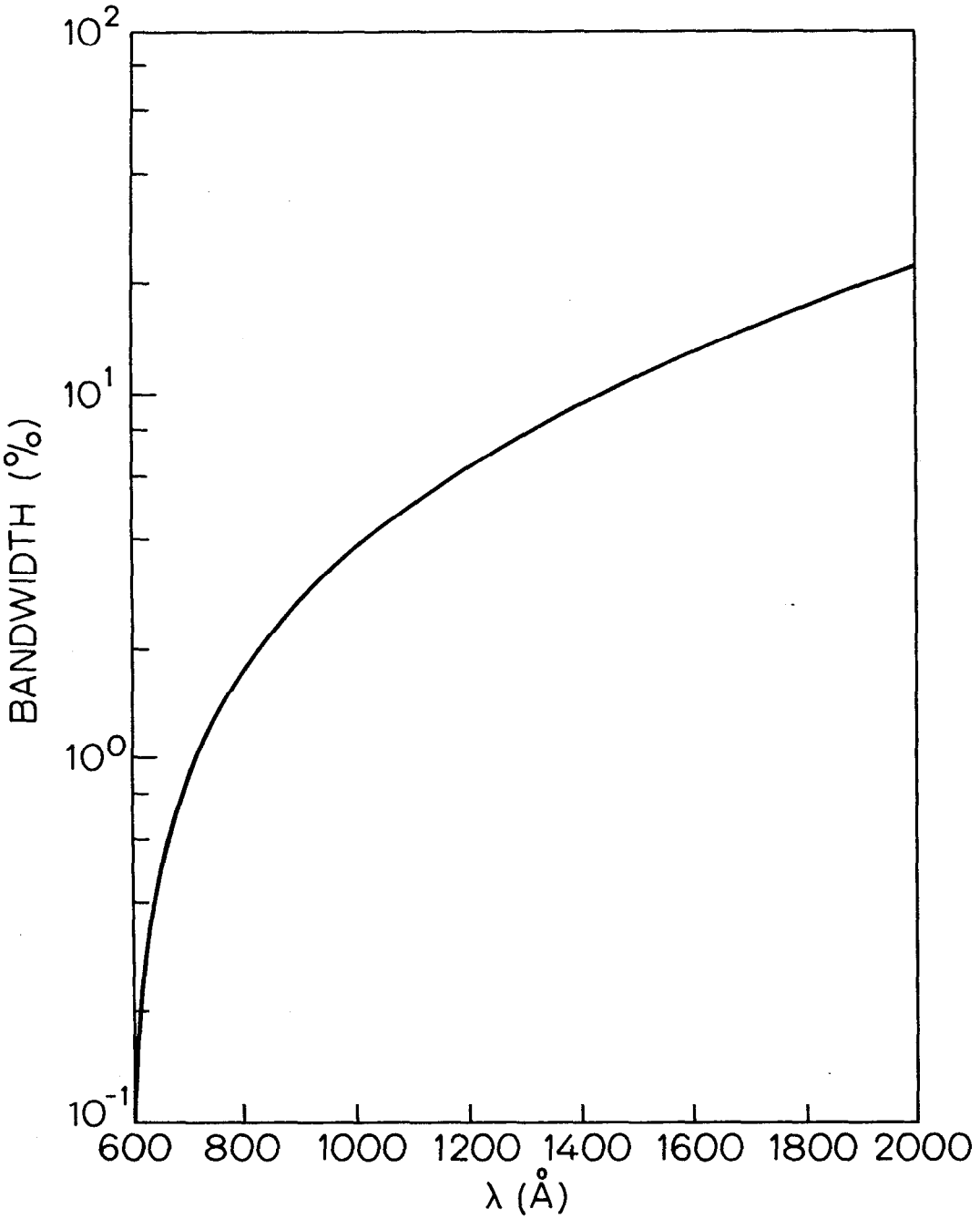
10^2
10^1
10^0
10^{-1}
BANDWIDTH (%)
600 800 1000 1200 1400 1600 1800 2000
λ (Å)

Fig. 4

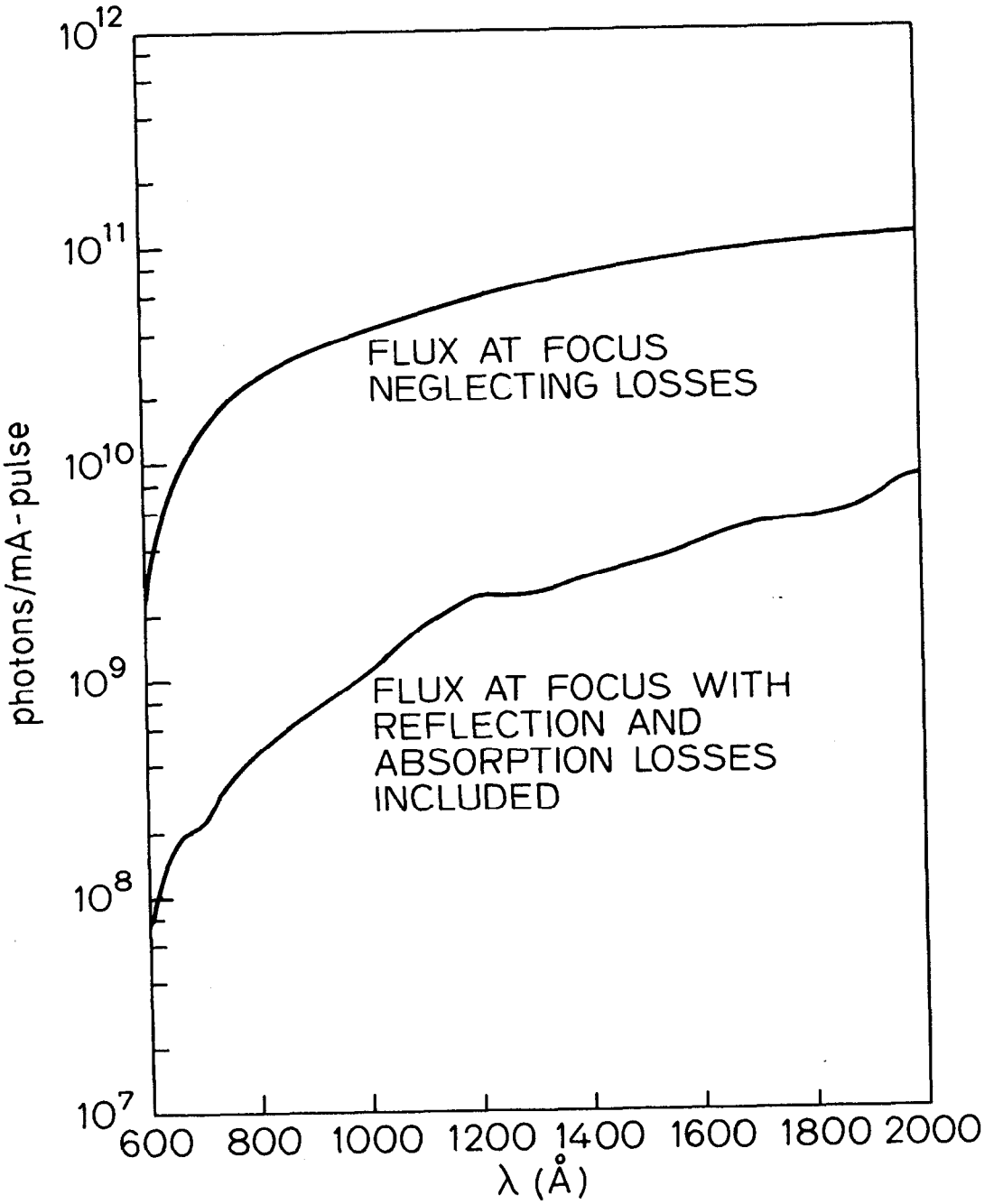
10^{12}
10^{11}
10^{10}
10^{9}
10^{8}
10^{7}
photons/mA-pulse
FLUX AT FOCUS
NEGLECTING LOSSES
FLUX AT FOCUS WITH
REFLECTION AND
ABSORPTION LOSSES
INCLUDED
600 800 1000 1200 1400 1600 1800 2000
λ (Å)

Fig. 5

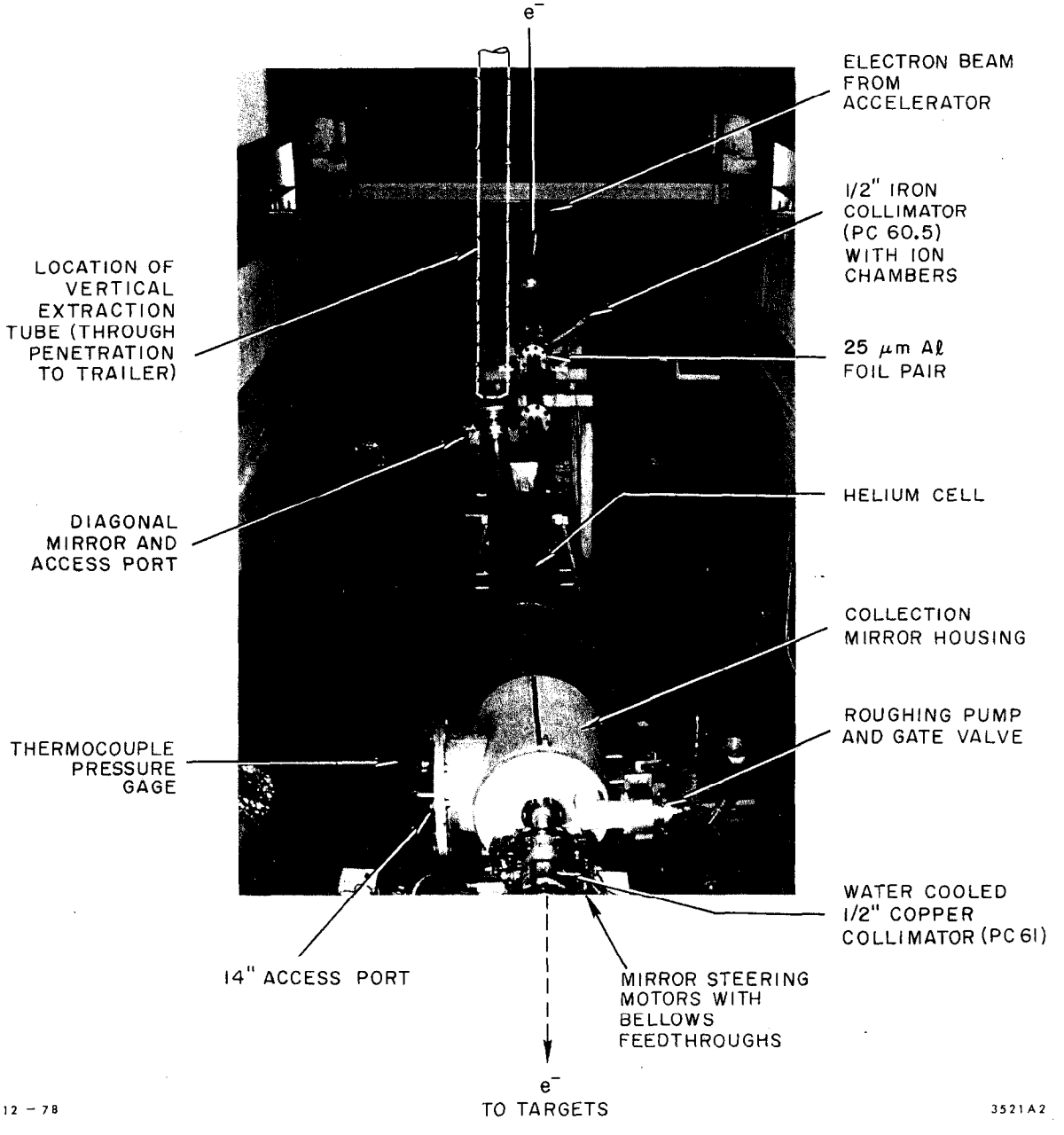
e⁻
ELECTRON BEAM FROM ACCELERATOR
1/2" IRON COLLIMATOR (PC 60.5) WITH ION CHAMBERS
LOCATION OF VERTICAL EXTRACTION TUBE (THROUGH PENETRATION TO TRAILER)
25 μm Aℓ FOIL PAIR
DIAGONAL MIRROR AND ACCESS PORT
HELIUM CELL
COLLECTION MIRROR HOUSING
THERMOCOUPLE PRESSURE GAGE
ROUGHING PUMP AND GATE VALVE
WATER COOLED 1/2" COPPER COLLIMATOR (PC 61)
14" ACCESS PORT
MIRROR STEERING MOTORS WITH BELLOWS FEEDTHROUGHS
e⁻
TO TARGETS
12 – 78
3521A2

Fig. 6

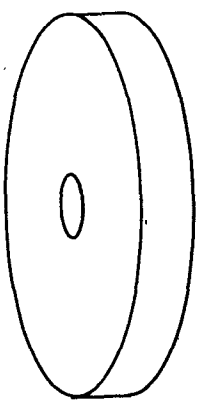

COLLECTION
MIRROR

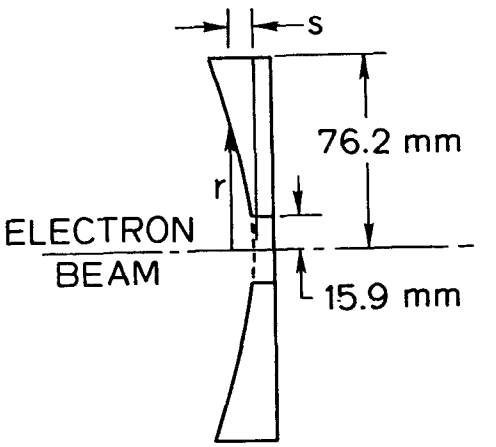

MIRROR CROSS-SECTION

Fig. 7

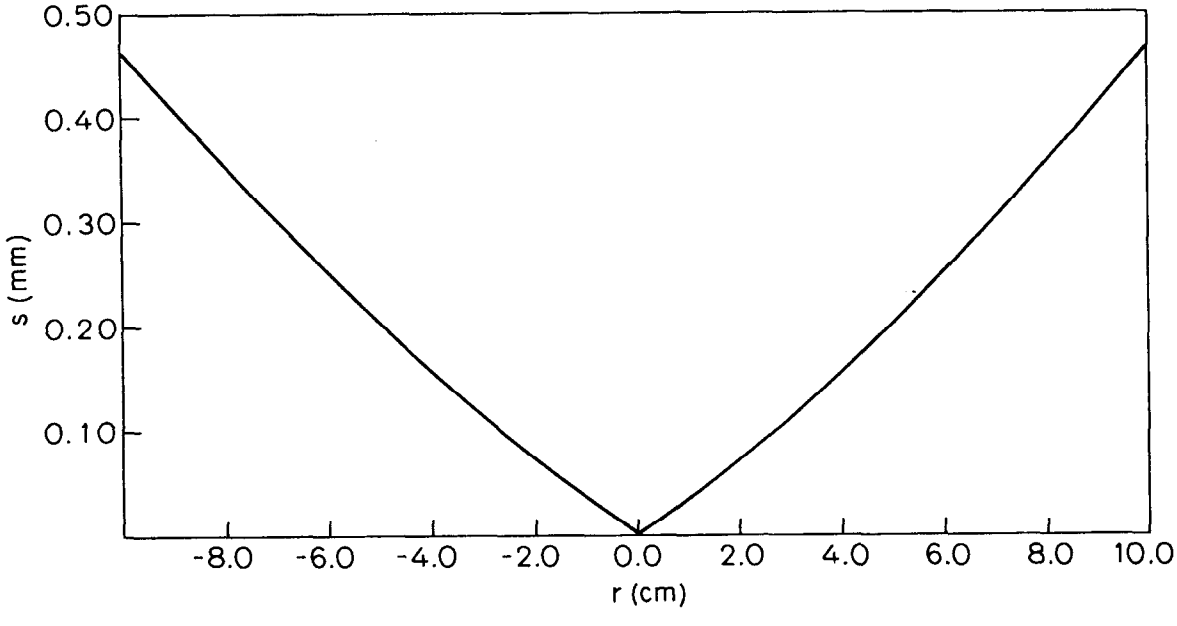

Fig. 8

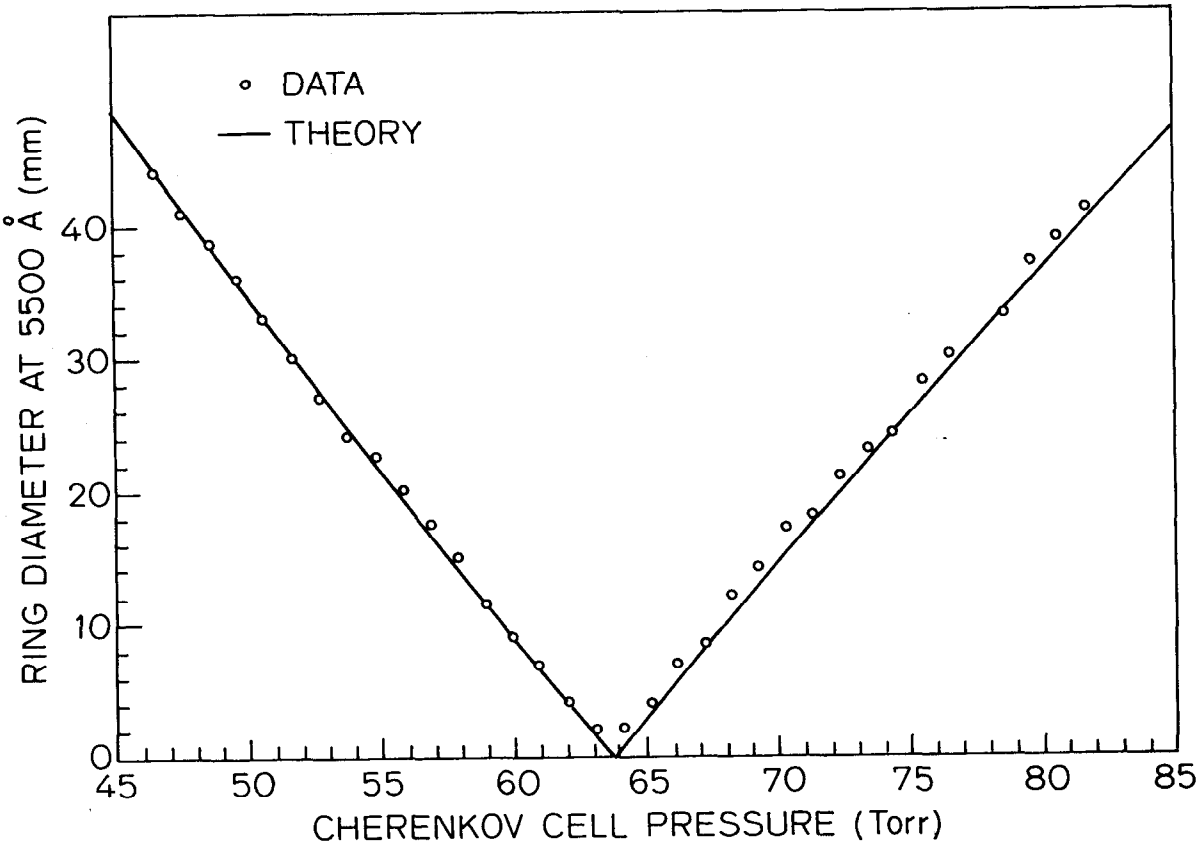
DATA
THEORY
RING DIAMETER AT 5500 Å (mm)
0
10
20
30
40
45
50
55
60
65
70
75
80
85
CHERENKOV CELL PRESSURE (Torr)

Fig. 9

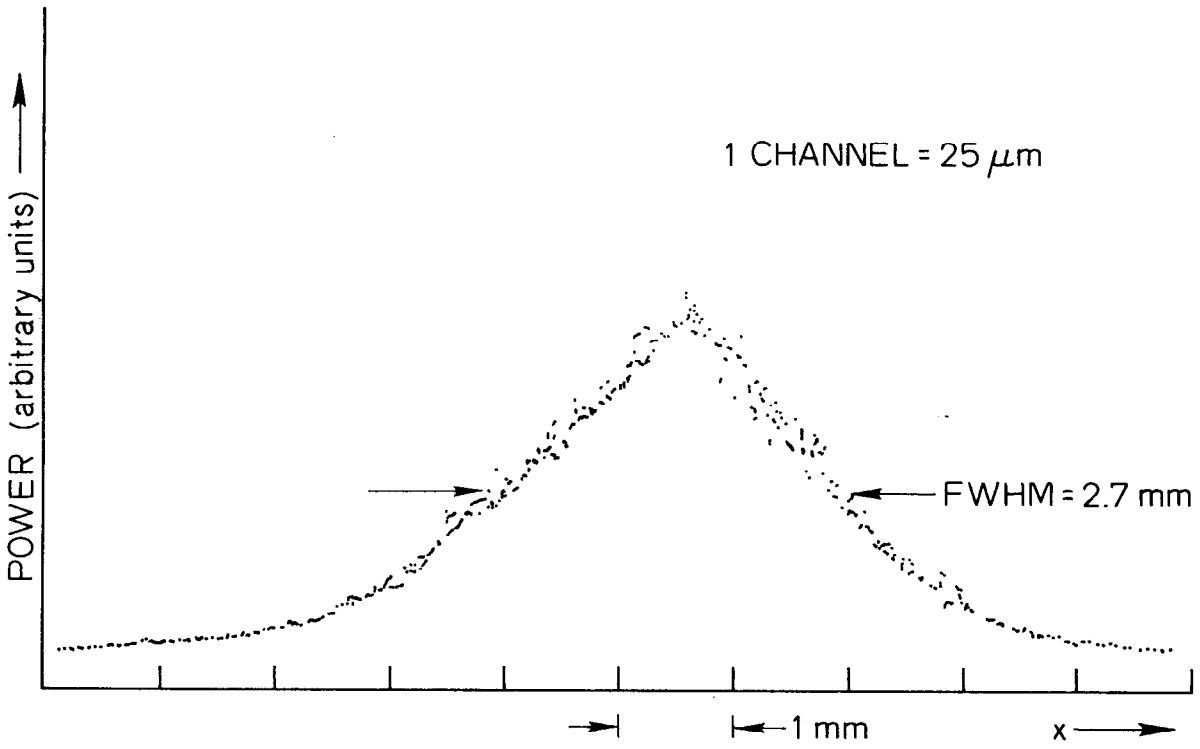

Fig. 10

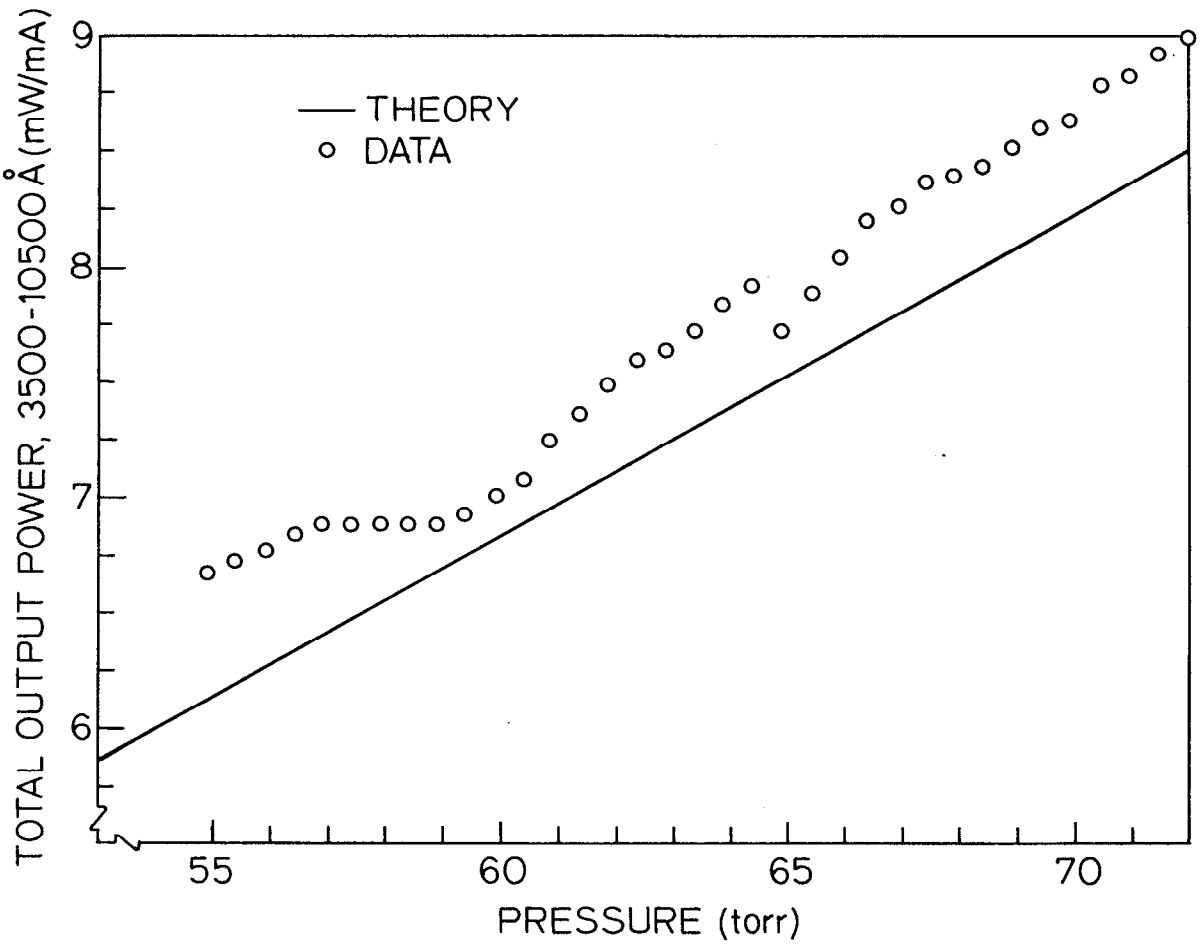
TOTAL OUTPUT POWER, 3500-10500 Å (mW/mA)
9
8
7
6
THEORY
DATA
55
60
65
70
PRESSURE (torr)

Fig. 11

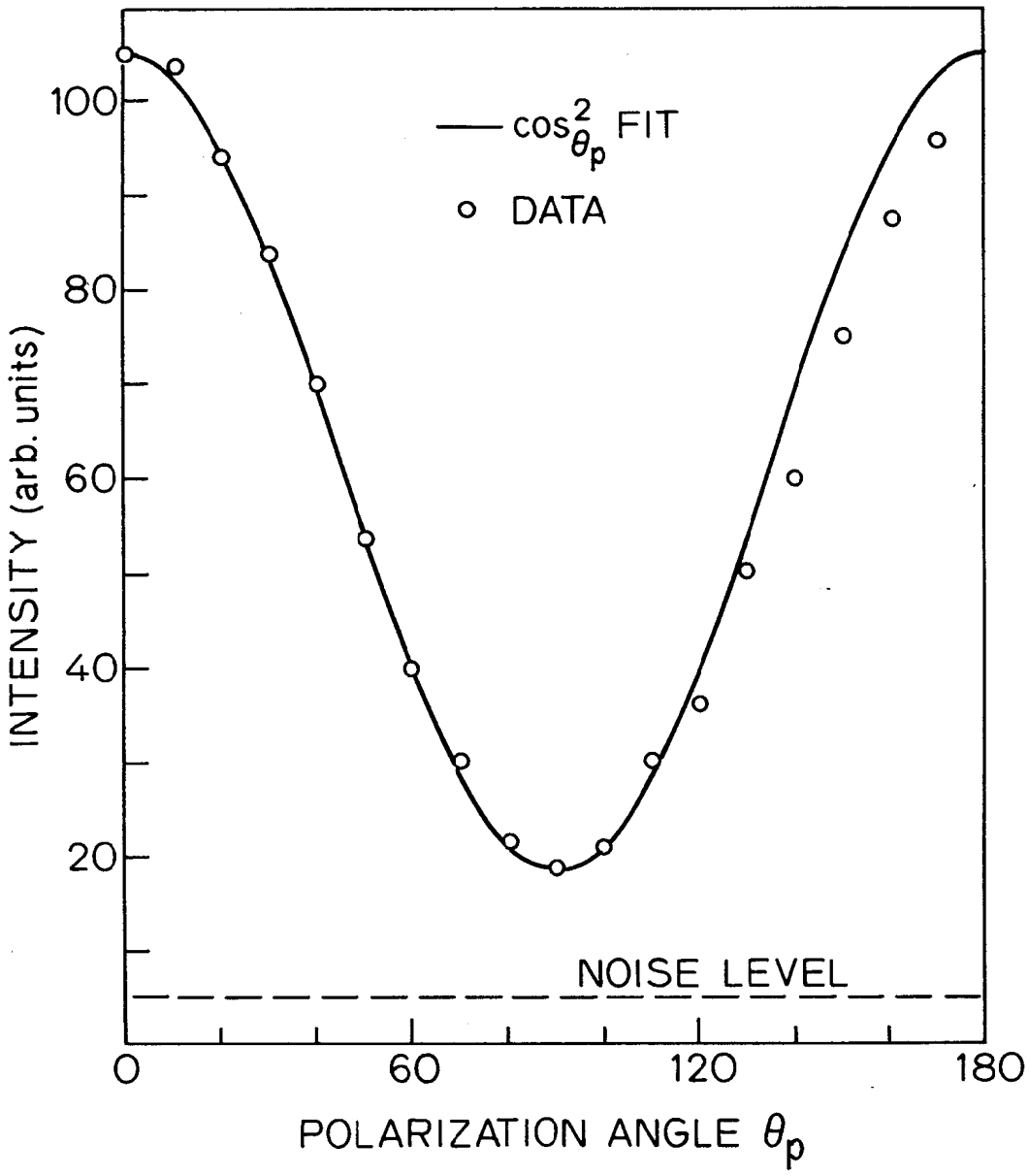
100
80
60
40
20
INTENSITY (arb. units)
$\cos^2\theta_p$ FIT
DATA
NOISE LEVEL
0
60
120
180
POLARIZATION ANGLE θ_p

Fig. 12